DFT Calculations for Structural, Electronic, and Magnetic Properties of ZnFe$_2$O$_4$ Spinel Oxide: The Role of Exchange-Correlation Functional

Anivaldo Ferreira de Rezende[a] , *Marisa Carvalho de Oliveira[b]** ,

Renan Augusto Pontes Ribeiro[c], Weber Duarte Mesquita[d], Jakelini de Jesus Marques[a] ,

Nilva Fernanda dos Santos Magalhães[a], Jorge Henrique Vieira Lemes[a], Elson Longo[b],

Maria Fernanda do Carmo Gurgel[a,d]

[a]*Universidade Federal de Catalão, Instituto de Química, Av. Dr. Lamartine Pinto de Avelar, 75704-020, Catalão, GO, Brasil.*
[b]*Universidade Federal de São Carlos, Centro de Desenvolvimento de Materiais Funcionais, 13565-905, São Carlos, SP, Brasil.*
[c]*Universidade do Estado de Minas Gerais, Departamento de Química, Av. 35501-170, Divinópolis, MG, Brasil.*
[d]*Universidade Federal de Catalão, Instituto de Física, Av. Dr. Lamartine Pinto de Avelar, 75704-020, Catalão, GO, Brasil.*

In this study, quantum-mechanical calculations in the framework of the Density Functional Theory (DFT) were performed to investigate the role of exchange-correlation functional in describing structural, electronic, and magnetic properties of ZnFe$_2$O$_4$. Herein B3LYP, PBE0, B1WC, and WC1LYP functionals implemented in the CRYSTAL17 code were considered due to the different amounts of the exact Hartree-Fock exchange fraction. In particular, the role of HF fraction on ZnFe$_2$O$_4$ properties was addressed for the first time. Indeed, structural, electronic, and magnetic properties indicate the dependence upon the exchange fraction, where WC1LYP with a 16% exact HF exchange exhibits the best performance compared to the other hybrid functionals. The obtained results reveal an excellent agreement for bandgap, local magnetic moment, long-range magnetic ordering, and unit-cell lattice parameters, overcoming previous theoretical studies based on local/semilocal exchange-correlation treatments. These results confirm the importance of hybrid HF/DFT with controlled HF term contribution to describe the essential features of strongly correlated materials.

Keywords: *ZnFe$_2$O$_4$, Antiferromagnetic, DFT, Exchange-correlation functional, WC1LYP.*

1. Introduction

The Zinc Ferrite (ZnFe$_2$O$_4$) is a solid oxide material with the normal spinel structure, where the Zn^{2+} occupies the tetrahedral sites, and the Fe^{3+} occupies the octahedral sites of the cubic Fd-3m structure[1]. It is an important material with special characteristics, showing chemical and thermal stability[2] with unique magnetic properties that enable applications such as gas sensors, electronic components, magnetic materials, and medical diagnosis and drug delivery[3]. Besides the other characteristics, the semiconductor behavior with a bandgap of ~1.9 eV is used in the photocatalysis of residual colored water. Due to his magnetic behavior, it can be easily removed after the process[4].

In the last decades, the first-principles calculations, mainly Density Functional Theory (DFT), have played a fundamental role in solid-state investigations, showing a reliable description for different properties[5-8]. The theoretical understanding of the ZnFe$_2$O$_4$ reported until now had applied

different computational methods to describe this material's structural and electronic properties in agreement with the experimental result. For instance, Yao et al.[9] confirmed the accuracy of the revised Perdew–Burke–Ernzerhof functional (RPBE), based on the Gradient Generalized Approximation (GGA), to investigate the effect of vacancies on the crystal and electronic structure in comparison to other GGA-based functionals. Rodríguez et al.[10] studied the stability, structural, electronic, and magnetic properties of the ZnFe$_2$O$_4$ surface (001) with DFT applying the Hubbard corrected PBE (PBE+U) approach. On the other hand, Fritsch[11] compared GGA+U and hybrid PBE0 formalism to investigate the electronic and optical properties of the material.

However, the obtained theoretical predictions for the magnetic properties of ZnFe$_2$O$_4$ did not approach the experimental results in most cases. In particular, the precise understanding of magnetic structure for spinel ferrites is exciting from the viewpoint of technological applications in several fields. The magnetic ground state definition can affect

the description of cation doping, structural, and magnetic phase transitions[9,12,13]. Indeed, the treatment of magnetic materials using DFT is challenging once the strong correlation generated from unpaired electrons should be balanced with the orbital localization. In commonly used Local-Density Approximation (LDA) or GGA exchange-correlation functionals, such refined treatment falls on the Self-Interaction Error (SIE) that provides a spurious interaction of an electron with itself, resulting in underestimated band gaps, erroneous localization for d–f orbitals, spin contamination, and the tendency toward magnetism[7,14]. Recently, a series of studies have involved a class of functional, which incorporates a fraction of the Hartree–Fock exchange on the DFT treatment to improve the description of strongly correlated materials denominated hybrid functional. Many hybrid functionals are described in the literature for different applications[14-17]. In particular, Zuo and co-workers deeply investigated the role of such exchange-correlation treatment on magnetic properties of different spinel ferrites, confirming that exact exchange fraction plays a vital role in the analysis of exchange coupling constant and magnetic properties[18-21].

In particular, in the present work, quantum-mechanical calculations performed for different hybrid (B3LYP, B1WC, PBE0, and WC1LYP) functionals were used to study the structural, electronic, and magnetic properties of $ZnFe_2O_4$, aiming to provide a general picture of the role of hybrid exchange-correlation treatment for this material. Moreover, the theoretical results reported here can guide the choice for exchange-correlation treatment of spinel ferrite materials, providing a reliable computational method to precisely predict and describe the structural, electronic, and mainly magnetic properties of such strongly correlated materials. The benchmarking analysis was based on the comparison between this paper (theoretical data) and previously reported experimental studies in the literature.

2. Computational Methods

Density functional theory (DFT) calculations using the B3LYP[22], B1WC[23], PBE0[24], and WC1LYP[25] exchange-correlation functional were carried out within CRYSTAL17 code[26] to investigate the structural, electronic, and magnetic properties for the $ZnFe_2O_4$ material. This method has been successfully employed for electronic, structural, photoluminescence, surface, morphology, and magnetic properties of several materials classes[27-31]. These exchange-correlation treatments were selected to consider the additional role of the exact Hartree-Fock exchange term in the description of correlated spins.

An atom-centered all-electron basis set described the Zn, Fe, and O atomic centers as 86-411d31G, 86-411d41G, and 8-411d1, respectively, according to the CRYSTAL basis set library. The XCrySDen program was used to analyze the $ZnFe_2O_4$ periodic model[32].

Here, $ZnFe_2O_4$ was simulated in a normal spinel configuration considering a conventional (56-atom) unit cell of the Fd-3m cubic symmetry, as illustrated in Figure 1a. In this normal structure, the Zn atoms are located at tetrahedral A-sites (Wyckoff position 8a (1/8, 1/8, 1/8)), whereas the Fe atoms (which carry a magnetic moment due to the partially filled 3d shell) occupy the octahedral B-sites (16d, (1/2, 1/2, 1/2)). The O atoms are at 32e (u,u,u) positions of the f.c.c. structure (u= 0.258[33] for the -3m origin). This methodology is in agreement with other theoretical studies published in the literature[34].

The crystalline structure was fully relaxed (in terms of atomic positions and cell lattice parameters) as a function of the total energy. The electronic integration over the Brillouin zone was performed using a 6×6×6 Monkhorst−Pack-mesh[35]. Five thresholds were chosen to control the accuracy of the Coulomb and exchange integral calculations (8, 8, 8, 8, and 14). The root-mean-square (RMS) gradient, RMS displacement,
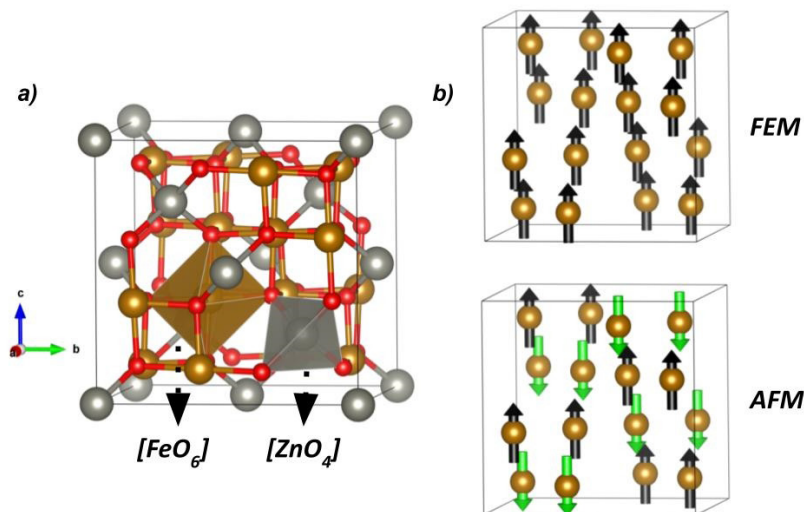

Figure 1. a) Schematic representation of conventional unit cell for crystalline structure for $ZnFe_2O_4$ in the normal spinel structure. The gray and orange polyhedral represent the $[ZnO_4]$ and $[FeO_6]$ clusters, respectively. b) Schematic representation of FEM and AFM magnetic models considering only open-shell Fe-sublattices.

DFT Calculations for Structural, Electronic, and Magnetic Properties of ZnFe₂O₄ Spinel Oxide: The Role of Exchange-Correlation Functional

3

maximum gradient, and maximum displacement were set to 3×10^{-4}, 1.2×10^{-3}, 4.5×10^{-4}, and 1.8×10^{-3} a.u., respectively.

The optimized crystalline structures were used to investigate the band structures and density of states (DOS) to explore the electronic structure of $ZnFe_2O_4$. The band structures were calculated for 30 k-points along the Γ (0; 0; 0), X (½, 0, ½), L (½, ½, ½), and Γ (0; 0; 0) high-symmetry points of the Brillouin zone.

The magnetic properties of $ZnFe_2O_4$ material were investigated by considering two collinear magnetic configurations (Figure 1b), defined as ferromagnetic (FEM) and antiferromagnetic (AFM), in agreement with other theoretical and experimental studies[34,36]. In this case, the magnetic models consider the interactions up to third neighbors, helping to describe the long-range magnetic ordering. The magnetic ground-state definition was based on the energy difference criteria between the investigated models.

Abbreviations are presented in the Supplementary Information.

3. Results and Discussion

3.1. Structural properties

The quantum-mechanical calculations in the framework of the Density Functional Theory (DFT optimized lattice parameters ($a = b = c$) of $ZnFe_2O_4$ agree with experimental results published in the literature as summarized in Table 1. The lowest lattice parameter was obtained using B1WC, and the highest values correspond to the B3LYP level of theory. In comparison to experimental data, all employed methods reasonably describe the crystalline structure of $ZnFe_2O_4$.

On the other hand, interesting trends were verified when comparing the hybrid functional results with previous theoretical calculations. For instance, previous theoretical calculations developed with semilocal GGA functional showed smaller lattice parameters when compared with hybrid functional or GGA+U approaches. The exception was found for B1WC, where the calculated results are very close to GGA. Moreover, the PBE0-CRYSTAL results reported here are closer to previous calculations with plane-wave basis

set within VASP[41], indicating good reproducibility of such hybrid exchange-correlation functional. Further, theoretical results obtained with B3LYP, PBE0, and WC1LYP were close to previous GGA+U calculations (U = 5.0[41] and U = 5.25 eV[11]). To select an adequate hybrid functional to describe $ZnFe_2O_4$ results, additional results concerning bandgap, magnetic ground-state, and local magnetic moment should be analyzed, as described in other sections.

3.2. Electronic properties

Electronic properties were investigated using Band structure with primary atomic orbitals (AOs), Mulliken Analysis Populations, Charge Density Maps, and partial projected DOS. Herein, the experimental AFM ground state was considered for the electronic structure analysis.

Figure 2a-d presents the calculated band structure for $ZnFe_2O_4$ obtained with different hybrid functional. The energy is in eV, and the Fermi Level was set at the maximum of the valence band (VBM). The dashed line represents the location of a Fermi level set as zero. The analyses of the principal atomic orbital (AOs) components of selected bands were performed with the ANBD option of the CRYSTAL17 code by using a threshold of 0.07 au for the important eigenvector coefficients following previous theoretical studies[42].

The E_{gap} value was obtained for all band structures as the difference between the valence band maximum (VBM) and the bottom of the conduction band (CBM). Once the VBM and CBM were located at Γ point for all investigated models, the minimal E_{gap} values correspond to a direct transition calculated as 2.61, 3.21, 4.06, and 2.53 eV for B1WC, B3LYP, PBE0, and WC1LYP hybrid functionals, respectively. Experimental bandgap results for $ZnFe_2O_4$ can be divided into two groups: (i) 1.78–2.01 eV obtained for mesoporous powder or nanoparticles and (ii) 2.61–3.25 eV reported for thin films and smaller nanoparticles, as reported by Ulpe et al.[43] and the references therein. However, comparing the hybrid DFT calculations reported here with previous theoretical data obtained with GGA+U (1.68 - 2.2 eV)[11,41,44,45] G_0W_0 (2.02 eV)[46] and PBE0 (3.68 eV)[11], it was observed that B1WC and WC1LYP hybrid functionals exhibit closer results to GGA+U and experimental data,

Table 1. Results for lattice parameter (Å), oxygen parameter (u), and bond distances (d_{Zn-O} and d_{Fe-O}) in (Å) for the B3LYP, B1WC, PBE0, and WC1LYP hybrid functionals. Additional sources of experimental and theoretical data were considered for comparative purposes.

| ZnFe₂O₄	$a = b = c$	u	d_{Zn-O}	d_{Fe-O}	Reference
B3LYP	8.521	0.261	2.003	2.042	This work
B1WC	8.398	0.260	1.969	2.016	This work
PBE0	8.449	0.261	1.987	2.024	This work
WC1LYP	8.470	0.260	1.986	2.033	This work
Experimental (nanoparticles)	8.430	0.259	-	-	Bock et al.[37]
Experimental (nanoparticles)	8.523	-	-	-	Oliveira et al.[38]
Experimental (Thin Films)	8.451	-	-	-	Jin et al.[39]
Experimental (nanoparticles)	8.434	-	-	-	Andhare et al.[40]
GGA	8.390	-	-	-	Jin et al.[39]
GGA	8.380	0.261	-	-	Quintero et al.[41]
GGA+U	8.457	0.260	-	-	Quintero et al.[41]
GGA+U	8.541	0.261	-	-	Fritsch[11]
PBE0	8.446	0.261	-	-	Fritsch[11]
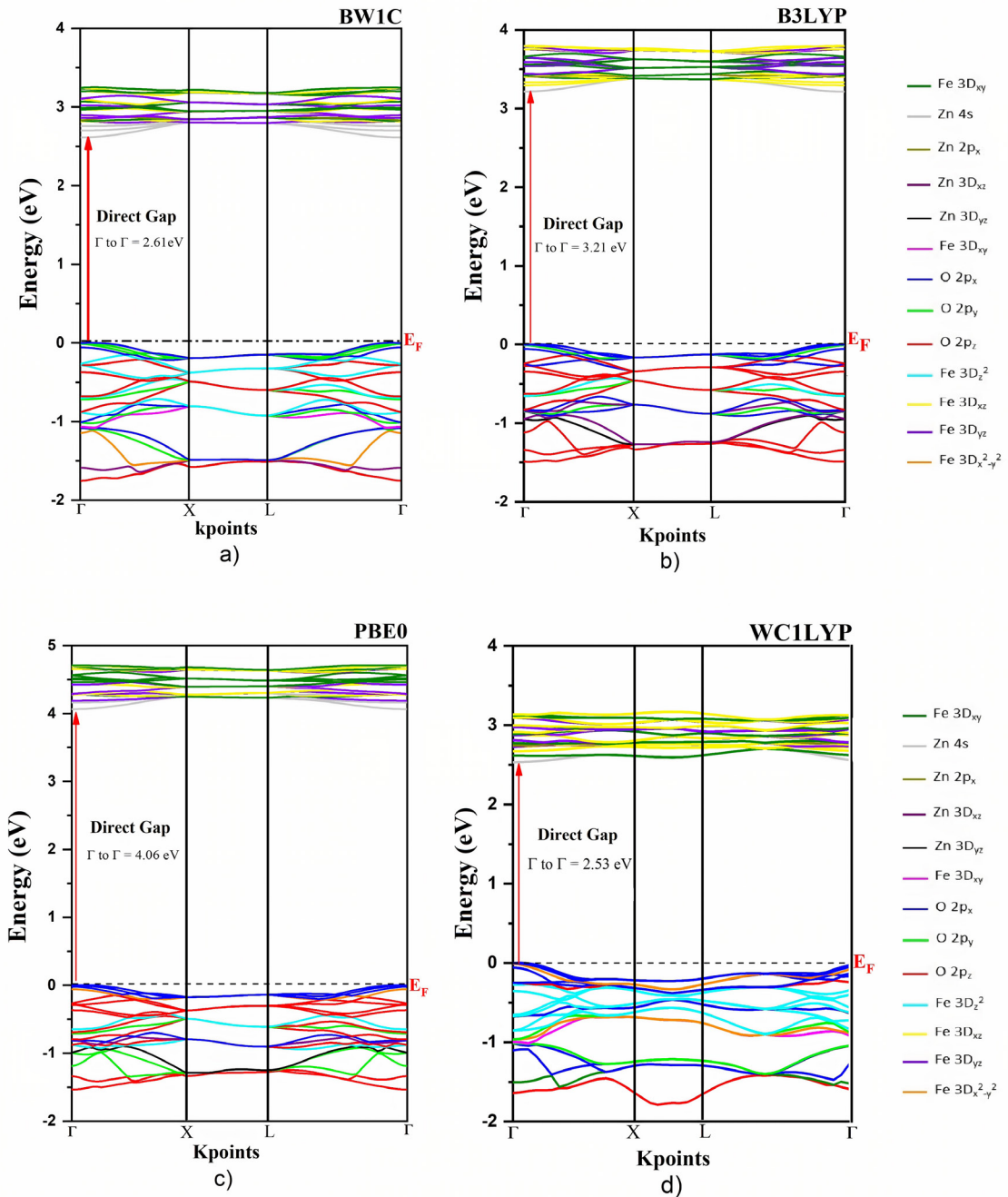
Figure 2. Representation of the ZnFe$_2$O$_4$ band structure with main atomic orbitals in VB and CB.

while B3LYP and PBE0 overestimate the bandgap value as a function of the Hartree-Fock fraction.

For all band structures, the VB is formed by O-2p states (2p$_x$, 2p$_y$, and 2p$_z$) atomic orbitals, with minor contributions from Fe-3d and Zn-3d atomic orbitals. The relative contributions of atomic orbitals for occupied and virtual bands depend upon the exchange-correlation treatment. In the VB, the Fe-3d$_z^2$ levels shift down to the O-2p$_x$ and O-2p$_z$ levels with a change of hybrid functional. In the B3LYP level, the top of VB has largely O-2p atomic orbitals,

while for WC1LYP, PBE0, and BW1C, the Fe-3d$_{x^2-y^2}$ and Fe3d$_z^2$ contributions become larger close to VBM. In CB, the main contribution for all approaches came from Fe-3d$_{xz}$ with a minor contribution of 3d-Zn atomic orbitals. These shifts are a consequence of the self-interaction correction provided by each hybrid functional.

The total and atom-resolved DOS projections, as shown in Figure 3, were analyzed to in-depth understand the role of atomic orbitals on the symmetry-adapted crystalline orbitals (SACO's). In this case, DOS analysis considered the VB
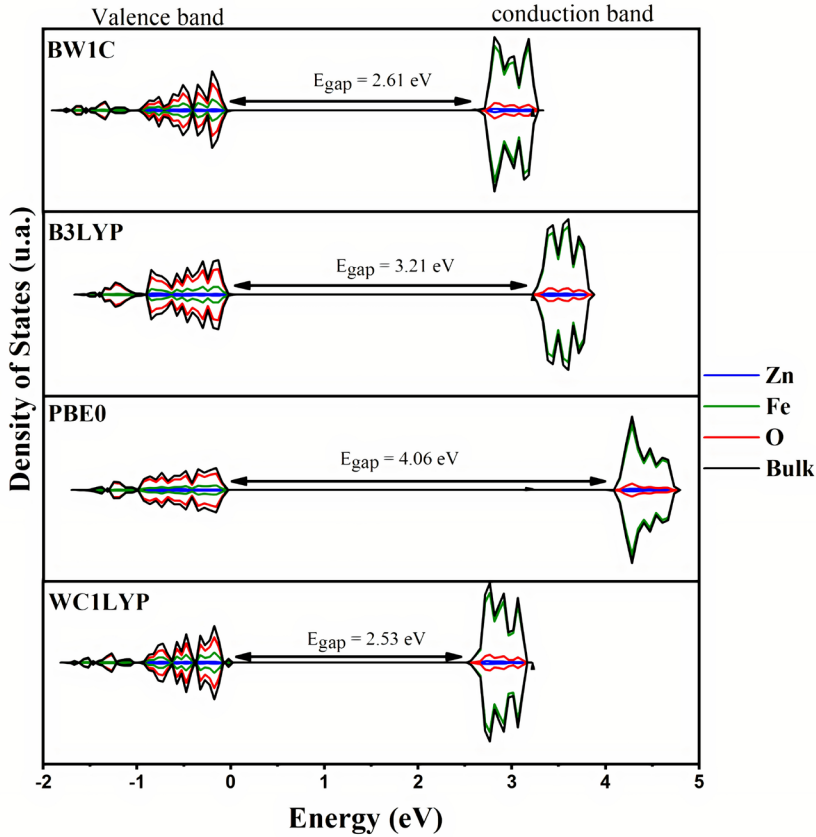
DFT Calculations for Structural, Electronic, and Magnetic Properties of ZnFe₂O₄ Spinel Oxide: The Role of
Exchange-Correlation Functional

5

Figure 3. Total and Partial Density of States (DOS) for ZnFe₂O₄, periodic models BW1C, B3LYP, PBE0, and WC1LYP hybrid functional.

SACO's located between 0 and -2 eV. The conduction band (CB) was analyzed with different energy ranges according to the employed hybrid functional. For BW1C, the CB was observed between 2.61 and 5 eV, B3LYP between 3.21 and 5 eV, PBE0 between 4.06 and 5 eV, and WC1YLP between 2.53 and 5 eV.

In the DOS analysis illustrated in Figure 3, the main contribution to VB, in all cases, was associated with O 2p (px, py, pz) orbitals with a small content of Zn and Fe orbitals. Concerning the conduction band (CB) composition, the obtained results indicate a dominant contribution of Fe 3d atomic orbitals ($3d_{xz}$, $3d_{xy}$, $3d_{yz}$, $3d_z^2$, $3d_{x^2-y^2}$) with a small content of Zn 3d atomic orbitals hybridized with oxygen atomic orbitals. Thus, it is possible to assume that an electron transfer inside the bandgap region should occur between 2p orbitals of the oxygen atom and 3d orbitals of the Fe and Zn in octal- and tetrahedral configuration, respectively, represented by [ZnO₄], and [FeO₆] clusters.

The electron density partition and its analogs (net charge and bonding population) correspond to a common characteristic used to analyze the nature of chemical bonds in ZnFe₂O₄. The Mulliken population analysis[47] was employed for both atomic charge and bonding overlap, as shown in Table 2 and Table 3, considering different hybrid exchange-correlation functionals.

Table 2. Theoretical results of the Mulliken population analysis for atomic charge net (in |e|) performed on ZnFe₂O₄ structure.

ZnFe₂O₄	B1WC	B3LYP	PBE0	WC1LYP
Atoms		Atomic charge (|e|)		
Zn	1.310	1.321	1.351	1.295
Fe	2.253	2.260	2.321	2.227
O	-1.454	-1.460	-1.498	-1.437

Table 3. Overlap population (in m|e|) of the Zn-O and Fe-O bonds in the AFM structure.

ZnFe₂O₄ bonds	B1WC	B3LYP	PBE0	WC1LYP
Zn-O	0.107	0.109	0.104	0.110
Fe-O	0.023	0.024	0.021	0.025

From Table 2, it can be seen positive charges on the Fe and Zn cations and negative charges on O anions. The O-atoms act as electron acceptors, whereas Zn and Fe atoms act as electron donors. Nevertheless, such theoretical results depend on the atomic basis set; then, the discussion about net charge will be performed through a qualitative viewpoint. The calculated charge for the O atoms was calculated following the formal charge O^{-2}, and the remaining values for Zn and Fe in the

tetra- and the octahedral site did not approach the formal values of +2 and +3, respectively.

The Mulliken bond population analysis is listed in Table 3. The positive values for Zn-O and Fe-O indicate the dominant covalent character due to the effective overlap of the atomic orbitals characterizing an accumulation of electronic density in the internuclear region. The PBE0 hybrid functional makes the materials more ionic due to the less value of the overlap population than other hybrid functional. On the other hand, the WC1LYP hybrid functional indicates a more covalent picture for all Zn-O and Fe-O bonds due to the larger overlap values.

The Zn-O and Fe-O bond character and charge distribution for the $ZnFe_2O_4$ periodic model were investigated using electronic density isolines in [001] direction (Figure 4). These results were obtained from the optimized wave function. An isoline is a set of equal-value points in domain data showing the electron density around the atomic nucleus. Colors can perform the charge density maps analysis plot in the plane to represent the charge density distribution. These electronic density maps were described along [001] direction containing Zn, O, and Fe atoms. This direction was chosen because it provides relevant information concerning the charge connection between $[ZnO_4]$ and $[FeO_6]$ tetra-octahedral clusters. The deviation from the ideal ionic charge density is more extensive for Zn than for Fe, suggesting a higher degree of covalent in the Zn-O than in the Fe-O interaction. The homogeneous distribution of contour lines represents the strongly covalent character in the interaction of the Zn and Fe cations atoms with oxygen anion on the [001] analyzed plane. The observed behavior occurs because of the hybridization between the 2p O atomic orbitals with 3d (Zn and Fe) atomic orbitals.

3.3. Magnetic properties

In this section, the magnetic properties of $ZnFe_2O_4$ were investigated by considering different hybrid exchange-correlation treatments on first-principles calculations. For this purpose, the local magnetic moment (S_z) was calculated for Fe-site and the energy difference of AFM and FEM models ($\Delta E_{AFM-FEM}$), as presented in Table 4.

The obtained results indicate that WC1LYP performs the best for both Fe-site magnetic moment and ground-state magnetic ordering representation. It is important to note that commonly employed B3LYP and PBE0 hybrid functional do not correctly describe the experimental AFM magnetic ordering for $ZnFe_2O_4$. On the other hand, the B1WC hybrid functional successfully described the AFM ground state with a larger magnetic moment than WC1LYP. Moreover, the WC1LYP overcomes GGA and GGA+U approaches once the computed magnetic moments showed a remarkable agreement with the experimental data and reported for bandgap analysis in the previous discussion.

Therefore, combining all analyses, it was possible to note that $ZnFe_2O_4$ properties depend upon the exchange-correlation treatment. The hybrid exchange-correlation formalism takes into account the mixing between the exact nonlocal Fock exchange and LDA/GGA exchange-correlation terms through
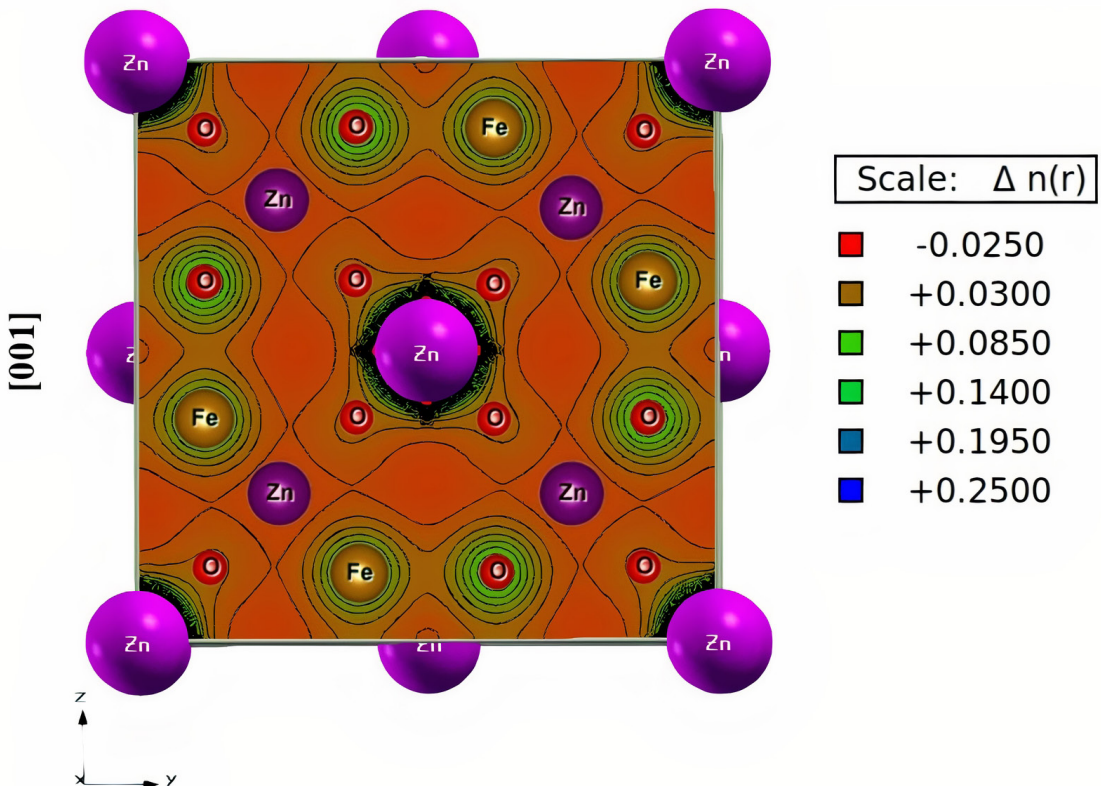

Figure 4. Electronic charge density for $ZnFe_2O_4$ in [001] direction using WC1LYP.

DFT Calculations for Structural, Electronic, and Magnetic Properties of $ZnFe_2O_4$ Spinel Oxide: The Role of Exchange-Correlation Functional

7

Table 4. Fe magnetic moment (S_z - μ_B) and $\Delta E_{AFM-FEM}$ (meV/f.u.) for $ZnFe_2O_4$ as a function of exchange-correlation treatment.

Exchange-Correlation Functional	S_z^{Fe}	$\Delta E_{AFM-FEM}$	Reference
B1WC	4.277	-25.94	This Work
B3LYP	4.297	18.24	This Work
PBE0	4.361	27.20	This Work
WC1LYP	4.254	-14.68	This Work
Experimental	4.220	AFM	Schiessl et al.[48]
PBE0	4.1 – 4.3	30.00	Fritsch[11]
GGA+U	4.1 – 4.2	AFM	Cheng[34]
GGA	3.7 – 3.9	AFM	Cheng[34]

the adiabatic connection (ACM) between non-interacting Kohn-Sham reference system ($\lambda = 0$) to the fully interacting real system ($\lambda = 1$). In this context, the dependence can be analyzed in terms of the Fock exchange fraction once the investigated functional contains different amounts of such term combined with different DFT formalisms.

For instance, the PBE0 functional contains the correlation energy fully described by the Perdew–Burke-Ernzerhof (PBE) formalism, while the exchange energy is obtained by combining 25% of Hartree–Fock exchange energy and 75% of PBE exchange functional[24], being described by the following expression:

$$E_{XC}^{PBE0} = \frac{1}{4} E_X^{HF} + \frac{3}{4} E_X^{PBE} + E_C^{PBE} \qquad (1)$$

On the other hand, commonly employed B3LYP uses the VWN local-density approximation and LYP functional for the correlation term, while the exchange term is described as combining Becke88 (B88), LSDA exchange functional with a 20% (a = 0.2) contribution of the exact Hartree-Fock exchange[49]. The such scheme takes into account three empirical parameters to rule the mixing of HF exchange and DFT exchange and correlation:

$$E_{XC}^{B3LYP} = (1-a) E_X^{LSDA} + a E_X^{HF} + b \Delta E_X^{B88} + c \Delta E_C^{LYP} + (1-c) E_C^{VWN} \qquad (2)$$

Moreover, B1WC mixes 16% (a = 0.16) of exact exchange energy with 84% of Wu-Cohen GGA exchange, with a PW91 correlation term[23]. The WC1LYP hybrid functional maintains the exchange description of B1WC, with the LYP functional for the correlation term[25]. In these cases, the one-coefficient representation is sufficient to rule the HF/DF exchange ratio according to:

$$E_{XC}^{B1WC} = (1-a) E_X^{WC-GGA} + a E_X^{HF} + E_C^{PW91} \qquad (3)$$

$$E_{XC}^{WC1LYP} = (1-a) E_X^{WC-GGA} + a E_X^{HF} + E_C^{LYP} \qquad (4)$$

Hence, it was observed that by reducing the exact Hartree-Fock exchange contribution, the structural, electronic, and magnetic properties of $ZnFe_2O_4$ materials become closer to the experimental results published in the

literature. This fact can be associated with the localization of unpaired electrons and the Fe 3d orbitals resulting in a strong correlation between the particles. Moreover, between B1WC and WC1LYP hybrid schemes, the latter becomes a more reliable choice to adequately describe the $ZnFe_2O_4$, mainly due to the contribution of LYP functional for energy levels distribution resulting in closer bandgap values for this treatment.

The role of the HF exchange term was confirmed by previous studies involving Fe-based materials and strongly correlated materials[50-52]. In particular, for Fe^{3+} 3d orbital description, the exact exchange fraction seems to play a fundamental role in analyzing exchange coupling constant and magnetic properties, highlighting the importance of benchmark analysis to describe the magnetic properties and electronic structure adequately[17-20]. Herein, it was confirmed that hybrid functional with reduced HF exchange term performs the best compared to previous studies based on LSDA+U and GGA+U schemes. Despite the worry about the computational cost involving hybrid functionals, CRYSTAL17 code can successfully perform the analysis of structural, electronic, and magnetic properties with an increased precision against the experimental with a reduced computational effort. Recently, the role of the exact exchange term was addressed as the inverse of the dielectric constant of solids, where the value can either be taken from experiments or estimated from first-principles calculations to follow the material dependency of the exchange-correlation functional[53,54]. This fact can be investigated in further studies comparing different exchange-correlation treatments to verify the compromise between the exchange fraction and the correlation treatment.

Those findings aim to fulfill the critical and lacking information about the proper benchmarking analysis of employed exchange-correlation treatments. Although the Hubbard corrections commonly employed along with GGA and LSDA treatments can give quite good results for the electronic properties of solid-state materials, the local magnetic moment, ground-state definitions, and related properties of strongly correlated cases remains challenging.

4. Conclusion

Hybrid Density Functional Theory calculations employing B3LYP, PBE0, B1WC, and WC1LYP exchange-correlation functional were carried out to investigate the structural, electronic, and magnetic properties of $ZnFe_2O_4$. The obtained results indicate the dependence of structural, electronic, and magnetic properties on the exact Hartree-Fock exchange fraction, being the WC1LYP the functional that best performs the investigated properties. In particular, the obtained theoretical results for this approach reveal an excellent agreement for bandgap, local magnetic moment, long-range magnetic ordering, and unit-cell lattice parameters concerning the experimental results published in the literature. Therefore, we can argue that hybrid HF/DFT formalism with controlled HF term contribution is the most suitable choice to investigate the strongly correlated $ZnFe_2O_4$, contributing to further studies involving such technological material. It is worth noting that the role of the HF-exchange term was addressed for the first time for $ZnFe_2O_4$, confirming that benchmarking analysis can overcome previous theoretical

studies and provide a guide for further studies of strongly correlated materials.

6. References

1. Boudjemaa A, Popescu I, Juzsakova T, Kebir M, Helaili N, Bachari K, et al. M-substituted (M = Co, Ni and Cu) zinc ferrite photo-catalysts for hydrogen production by water photo-reduction. Int J Hydrogen Energy. 2016;41(26):11108-18.

2. Liu H, Guo Y, Zhang Y, Wu F, Liu Y, Zhang D. Synthesis and properties of $ZnFe_2O_4$ replica with biological hierarchical structure. Mater Sci Eng B. 2013;178(16):1057-61.

3. Jia Z, Ren D, Liang Y, Zhu R. A new strategy for the preparation of porous zinc ferrite nanorods with subsequently light-driven photocatalytic activity. Mater Lett. 2011;65(19-20):3116-9.

4. Guo X, Zhu H, Li Q. Visible-light-driven photocatalytic properties of $ZnO/ZnFe_2O_4$ core/shell nanocable arrays. Appl Catal B. 2014;160–161:408-14.

5. Varignon J, Bristowe NC, Bousquet E, Ghosez P. Magneto-electric multiferroics: designing new materials from first-principles calculations. Physical Sciences Reviews. 2020;5(2):20190069.

6. Goffinet M, Hermet P, Bilc DI, Ghosez P. Hybrid functional study of prototypical multiferroic bismuth ferrite. Phys Rev B Condens Matter Mater Phys. 2009;79(1):014403.

7. Ribeiro RAP, de Lazaro SR, Gatti C. The role of exchange–correlation functional on the description of multiferroic properties using density functional theory: the $ATiO_3$ (A = Mn, Fe, Ni) case study. RSC Advances. 2016;6(103):101216-25.

8. Jain A, Hautier G, Moore CJ, Ping Ong S, Fischer CC, Mueller T, et al. A high-throughput infrastructure for density functional theory calculations. Comput Mater Sci. 2011;50(8):2295-310.

9. Yao J, Li Y, Li X, Zhu X. First-principles study of the geometric and electronic structures of zinc ferrite with vacancy defect. Metall Mater Trans, A Phys Metall Mater Sci. 2016;47(7):3753-60.

10. Rodríguez KLS, Quintero JJM, Medina Chanduví HH, Rebaza AVG, Faccio R, Adeagbo WA, et al. Ab-initio approach to the stability and the structural, electronic and magnetic properties of the (001) $Znfe_2O_4$ surface terminations. Appl Surf Sci. 2020;499:143859.

11. Fritsch D. Electronic and optical properties of spinel zinc ferrite: ab initio hybrid functional calculations. J Phys Condens Matter. 2018;30(9):095502.

12. Bohra M, Alman V, Arras R. Nanostructured $ZnFe_2O_4$: an exotic energy material. Nanomaterials (Basel). 2021;11(5):1286.

13. Salcedo Rodríguez KL, Stewart SJ, Mendoza Zélis PM, Pasquevich GA, Rodríguez Torres CE. Role of defects on

14. Ribeiro RAP, de Lazaro SR, Pianaro SA. Density Functional Theory applied to magnetic materials: Mn_3O_4 at different hybrid functionals. J Magn Magn Mater. 2015;391:166-71.

15. Hafner J, Wolverton C, Ceder G. Toward computational materials design: the impact of density functional theory on materials research. MRS Bull. 2006;31(9):659-68.

16. Chen Z-Y, Yang J-L. The B3LYP hybrid density functional study on solids. Front Phys China. 2006;1(3):339-43.

17. Muscat J, Wander A, Harrison NM. On the prediction of band gaps from hybrid functional theory. Chem Phys Lett. 2001;342(3-4):397-401.

18. Zuo X, He Y, Yang A, Bernardo B, Harris VG, Vittoria C. Calculation of exchange constants in spinel ferrites with magnetic S-state ions. J Appl Phys. 2005;97(10):10F104.

19. Zuo X, Yang A, Vittoria C, Harris VG. Computational study of copper ferrite ($CuFe_2O_4$). J Appl Phys. 2006;99(8):08M909.

20. Zuo X, Yan S, Barbiellini B, Harris VG, Vittoria C. A computational study of nickel ferrite. J Magn Magn Mater. 2006;303(2):e432-5.

21. Zuo X, Vittoria C. Calculation of exchange integrals and electronic structure for manganese ferrite. Phys Rev B Condens Matter Mater Phys. 2002;66(18):184420.

22. Stephens PJ, Devlin FJ, Chabalowski CF, Frisch MJ. Ab initio calculation of vibrational absorption and circular dichroism spectra using density functional force fields. J Phys Chem. 1994;98(45):11623-7.

23. Bilc DI, Orlando R, Shaltaf R, Rignanese G-M, Íñiguez J, Ghosez P. Hybrid exchange-correlation functional for accurate prediction of the electronic and structural properties of ferroelectric oxides. Phys Rev B Condens Matter Mater Phys. 2008;77(16):165107.

24. Adamo C, Barone V. Toward reliable density functional methods without adjustable parameters: the PBE0 modelThe. J Chem Phys. 1999;110(13):6158-70.

25. Demichelis R, Civalleri B, Ferrabone M, Dovesi R. On the performance of eleven DFT functionals in the description of the vibrational properties of aluminosilicates: performance of eleven DFT functionals. Int J Quantum Chem. 2010;110(2):406-15.

26. Dovesi R, Erba A, Orlando R, Zicovich-Wilson CM, Civalleri B, Maschio L, et al. Quantum-mechanical condensed matter simulations with CRYSTAL. Wiley Interdiscip Rev Comput Mol Sci. 2018;8(4):e1360.

27. Mesquita WD, Jesus SR, Oliveira MC, Ribeiro RAP, de Cássia Santos MR, Godinho M Jr, et al. Barium strontium titanate-based perovskite materials from DFT perspective: assessing the structural, electronic, vibrational, dielectric and energetic properties. Theor Chem Acc. 2021;140(3):27.

28. Mesquita WD, Santos MRDC, Espinosa JWM, Leal SHB S, Longo E, Gurgel MFDC. Theoretical study of the structural properties of the lead titanate doped with strontium. Orbital. 2019;11(2):91-6.

29. Santiago AAG, Oliveira MC, Ribeiro RAP, Tranquilin RL, Longo E, Lázaro SR, et al. Atomistic perspective on the intrinsic white-light photoluminescence of rare-earth free $MgMoO_4$ nanoparticles. Cryst Growth Des. 2020;20(10):6592-603.

30. Ribeiro RAP, Oliveira MC, Bomio MRD, de Lazaro SR, Andrés J, Longo E. Connecting the surface structure, morphology and photocatalytic activity of Ag_2O: an in depth and unified theoretical investigation. Appl Surf Sci. 2020;509:145321.

31. Manjunatha K, Jagadeesha Angadi V, Ribeiro RAP, Longo E, Oliveira MC, Bomio MRD, et al. Structural, electronic, vibrational and magnetic properties of Zn^{2+} substituted $MnCr_2O_4$ nanoparticles. J Magn Magn Mater. 2020;502:166595.

32. Kokalj A. XCrySDen-a new program for displaying crystalline structures and electron densities. J Mol Graph Model. 1999;17(3-4):176-9.

the magnetic behaviour of the geometrically frustrated spinel $ZnFe_2O_4$. J Alloys Compd. 2018;752:289-95.

DFT Calculations for Structural, Electronic, and Magnetic Properties of ZnFe$_2$O$_4$ Spinel Oxide: The Role of Exchange-Correlation Functional

9

33. Gomes JA, Sousa MH, Tourinho FA, Mestnik-Filho J, Itri R, Depeyrot J. Rietveld structure refinement of the cation distribution in ferrite fine particles studied by X-ray powder diffraction. J Magn Magn Mater. 2005;289:184-7.

34. Cheng C. Long-range antiferromagnetic interactions in ZnFe$_2$O$_4$ and CdFe$_2$O$_4$: density functional theory calculations. Phys Rev B Condens Matter Mater Phys. 2008;78(13):132403.

35. Monkhorst HJ, Pack JD. Special points for Brillouin-zone integrations. Phys Rev B. 1976;13(12):5188-92.

36. Yamada Y, Kamazawa K, Tsunoda Y. Interspin interactions in ZnFe$_2$O$_4$: theoretical analysis of neutron scattering study. Phys Rev B Condens Matter Mater Phys. 2002;66(6):064401.

37. Bock DC, Tallman KR, Guo H, Quilty C, Yan S, Smith PF, et al. De)lithiation of spinel ferrites Fe$_3$O$_4$, MgFe$_2$O$_4$, and ZnFe$_2$O$_4$: a combined spectroscopic, diffraction and theory study. Phys Chem Chem Phys. 2020;22(45):26200-15.

38. Oliveira RC, Ribeiro RAP, Cruvinel GH, Ciola Amoresi RA, Carvalho MH, Aparecido de Oliveira AJ, et al. Role of surfaces in the magnetic and ozone gas-sensing properties of ZnFe$_2$O$_4$ nanoparticles: theoretical and experimental insights. ACS Appl Mater Interfaces. 2021;13(3):4605-17.

39. Jin C, Li P, Mi W, Bai H. Structure, magnetic, and transport properties of epitaxial ZnFe$_2$O$_4$ films: an experimental and first-principles study. J Appl Phys. 2014;115(21):213908.

40. Andhare DD, Jadhav SA, Khedkar MV, Somvanshi SB, More SD, Jadhav KM. Structural and chemical properties of ZnFe$_2$O$_4$ nanoparticles synthesised by chemical co-precipitation technique. J Phys Conf Ser. 2020;1644(1):012014.

41. Quintero JJ, Torres CE, Errico LA. Ab initio calculation of structural, electronic and magnetic properties and hyperfine parameters at the Fe sites of pristine ZnFe$_2$O$_4$. J Alloys Compd. 2018;741:746-55.

42. Rosa ILV, Oliveira MC, Assis M, Ferrer M, André RS, Longo E, et al. A theoretical investigation of the structural and electronic properties of orthorhombic CaZrO$_3$. Ceram Int. 2015;41(2):3069-74.

43. Ulpe AC, Bauerfeind KCL, Granone LI, Arimi A, Megatif L, Dillert R, et al. Photoelectrochemistry of ferrites: theoretical predictions vs. Experimental results. Z Phys Chem. 2020;234(4):719-76.

44. O'Brien CJ, Rák Z, Brenner DW. Free energies of (Co, Fe, Ni, Zn)Fe$_2$O$_4$ spinels and oxides in water at high temperatures and pressure from density functional theory: results for stoichiometric NiO and NiFe$_2$O$_4$ surfaces. J Phys Condens Matter. 2013;25(44):445008.

45. Andersson DA, Stanek CR. Mixing and non-stoichiometry in Fe-Ni-Cr-Zn-O spinel compounds: density functional theory calculations. Phys Chem Chem Phys. 2013;15(37):15550-64.

46. Ziaei V, Bredow T. Ab-initio optical properties and dielectric response of open-shell spinel zinc ferrite. Eur Phys J B. 2017;90(2):29.

47. Mulliken R. Theoretical studies of icosahedral C60 and some related species. J Chem Phys. 1955;23:10-1063.

48. Schiessl W, Potzel W, Karzel H, Steiner M, Kalvius GM, Martin A, et al. Magnetic properties of the ZnFe$_2$O$_4$ spinel. Phys Rev B Condens Matter. 1996;53(14):9143-52.

49. Lee C, Yang W, Parr RG. Development of the Colle-Salvetti correlation-energy formula into a functional of the electron density. Phys Rev B Condens Matter. 1988;37(2):785-9.

50. Yazdani-Kachoei M, Jalali-Asadabadi S, Ahmad I, Zarringhalam K. Pressure dependency of localization degree in heavy fermion CeIn$_3$: a density functional theory analysis. Sci Rep. 2016;6(1):31734.

51. Liyanage LSI, Kim S, Hong Y-K, Park J-H, Erwin SC, Kim S-G. Theory of magnetic enhancement in strontium hexaferrite through Zn–Sn pair substitution. J Magn Magn Mater. 2013;348:75-81.

52. Meng Y, Liu X-W, Huo C-F, Guo W-P, Cao D-B, Peng Q, et al. When density functional approximations meet iron oxides. J Chem Theory Comput. 2016;12(10):5132-44.

53. Skone JH, Govoni M, Galli G. Self-consistent hybrid functional for condensed systems. Phys Rev B Condens Matter Mater Phys. 2014;89(19):195112.

54. Marques MAL, Vidal J, Oliveira MJT, Reining L, Botti S. Density-based mixing parameter for hybrid functionals. Phys Rev B Condens Matter Mater Phys. 2011;83(3):035119.